

# Highly Efficient Near IR Photosensitizers Based-on Ir-C Bonded Porphyrin-Aza-BODIPY Conjugates

Jinfeng Zhou,<sup>a</sup> Lizhi Gai,<sup>b</sup> Zhikuan Zhou,<sup>a</sup> John Mack,<sup>c,\*</sup> Hailin Qiu,<sup>a</sup> Kin Shing Chanb,<sup>\*</sup> and Zhen Shena,<sup>\*</sup> Kejing Xu,<sup>d</sup> Jianzhang Zhao,<sup>d</sup>

## Table of contents

### Supplementary data

- Figure S1.  $^1\text{H}$  NMR spectrum (400 MHz) of **1a** in  $\text{C}_6\text{D}_6$ .
- Figure S2.  $^{13}\text{C}$  NMR spectrum (175 MHz) of **1a** in  $\text{C}_6\text{D}_6$ .
- Figure S3.  $^1\text{H}$  NMR spectrum (400 MHz) of **1b** in  $\text{C}_6\text{D}_6$ .
- Figure S4.  $^{13}\text{C}$  NMR spectrum (175 MHz) of **1b** in  $\text{C}_6\text{D}_6$ .
- Table S1 Spectral data in different solvents.
- Figure S5. TD-DFT calculations calculated in the presence of dichloromethane.
- Figure S6. MO energies of **Ir<sup>III</sup>(ttP)Ph** (1), **aza-BODIPY-a** (2), **aza-BODIPY-b** (3), **1a** (4) and **1b** (5) in TD-DFT calculations calculated in the presence of dichloromethane.
- Figure S7. a) Absorption spectra of DPBF upon irradiation ( $\lambda_{\text{irr}} = 671$  nm) with 30 s interval in the presence of 4.5  $\mu\text{M}$  **aza-BODIPY-a**; b) Absorption spectra of DPBF upon irradiation ( $\lambda_{\text{irr}} = 671$  nm) with 30 s interval in the presence of MB; c) Plot of the change in absorbance of DPBF at 410 nm versus irradiation time in the presence of **aza-BODIPY-a** against MB as a standard in air-saturated dichloromethane.
- Figure S7. The  $^1\text{O}_2$  phosphorescence spectra of **aza-BODIPY-a** in air-saturated dichloromethane upon irradiation with 650 nm ( $c = 4.5 \mu\text{M}$ , 298 K).
- Figure S9. The  $^1\text{O}_2$  phosphorescence spectra of **Ir<sup>III</sup>(ttP)Ph** in air-saturated dichloromethane upon irradiation with 405 nm (red) and 690 nm (black) ( $c = 5.0 \mu\text{M}$ , 298 K).
- Figure S10. The  $^1\text{O}_2$  phosphorescence spectra of **1a** ( $c = 5.0 \mu\text{M}$ ) and **1b** ( $c = 5.0 \mu\text{M}$ ) in air-saturated dichloromethane upon irradiation with 405 (red) and 690 nm (black) laser light at room temperature.

**Table S2.** The ratios of singlet oxygen quantum yields ( $\Phi_{\Delta}$ ) upon irradiation with 405 nm and 690 nm of **1a**, **1b** in O<sub>2</sub> saturated dichloromethane at 298 K.

## Supplementary data

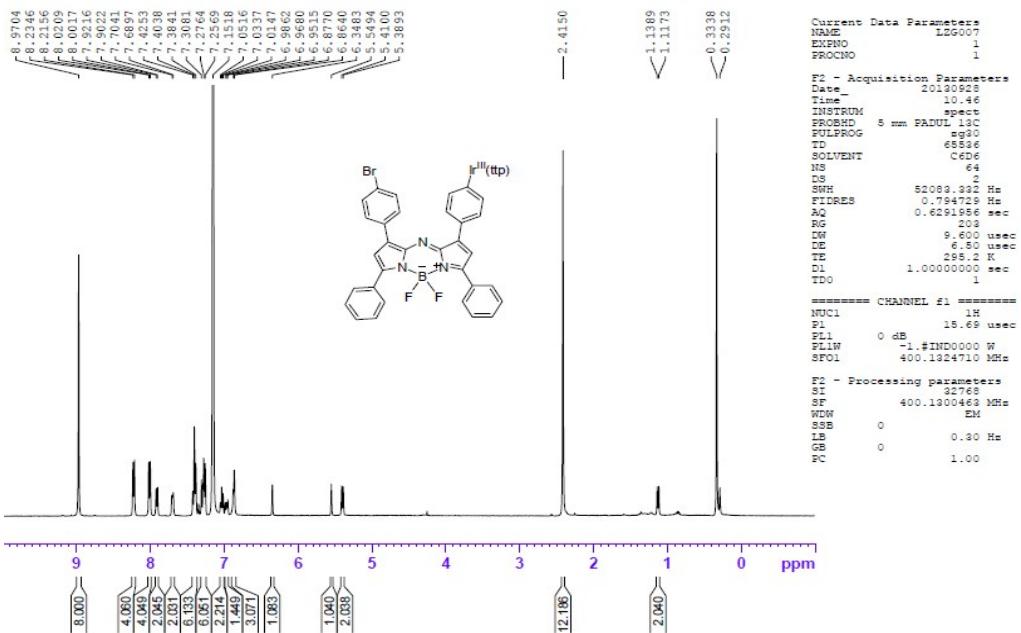


**Figure S1.**  $^1\text{H}$  NMR spectrum (400 MHz) of **1a** in  $\text{C}_6\text{D}_6$ .

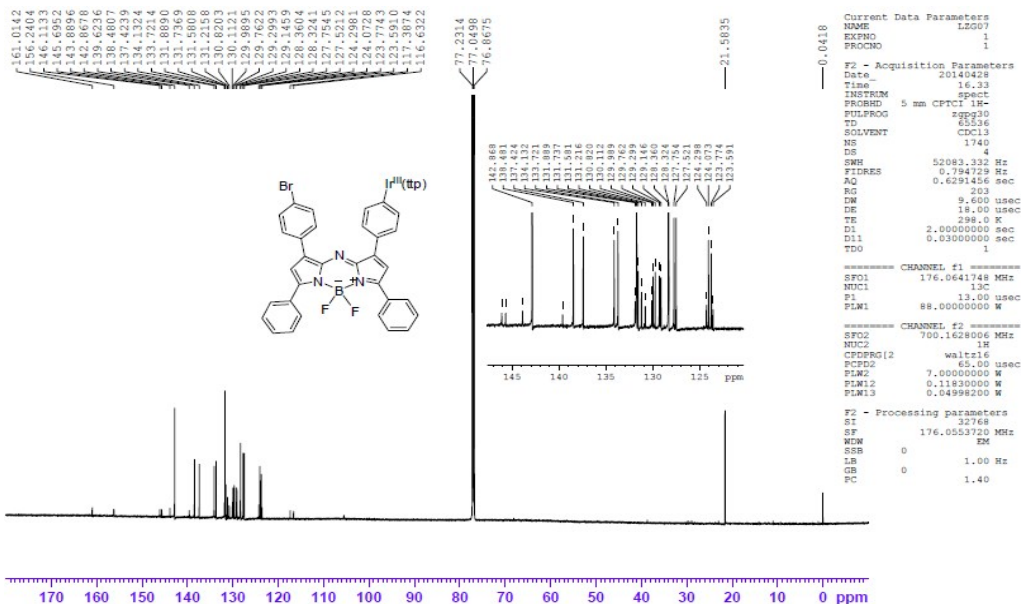


**Figure S2.**  $^{13}\text{C}$  NMR spectrum (175 MHz) of **1a** in  $\text{C}_6\text{D}_6$ .

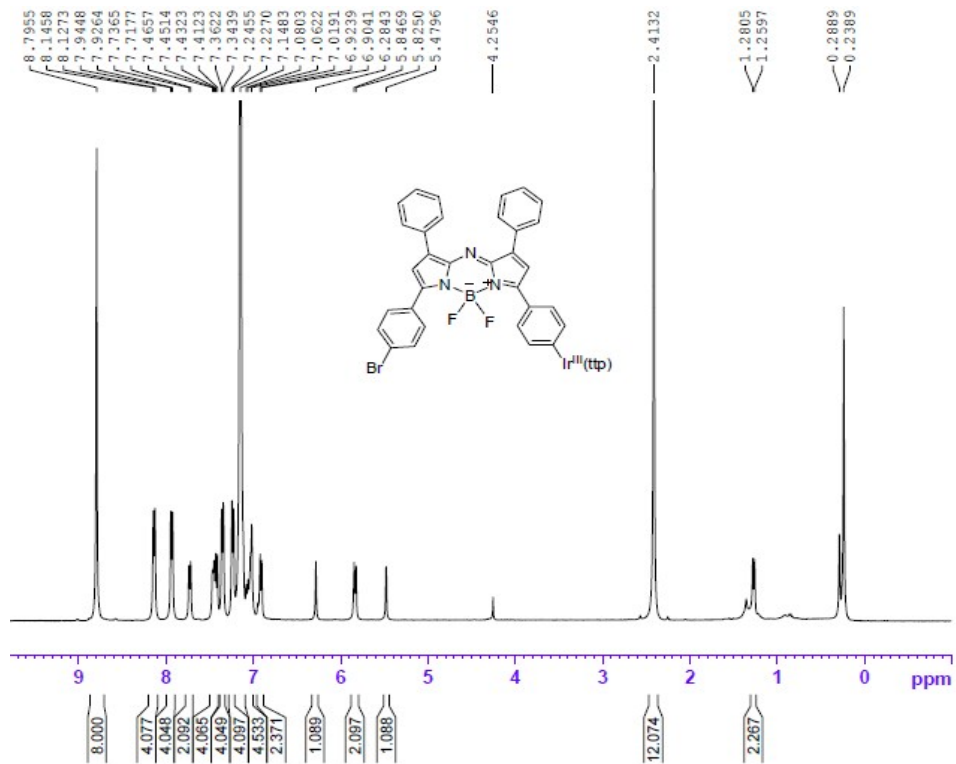


**Figure S3.**  $^1\text{H}$  NMR spectrum (400 MHz) of **1b** in  $\text{C}_6\text{D}_6$ .

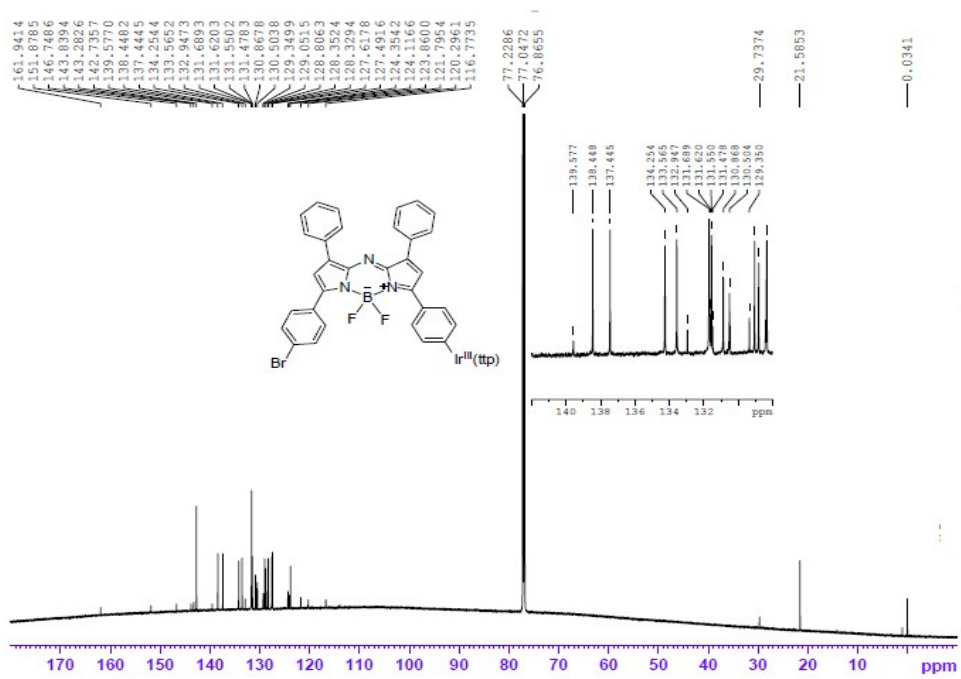


**Figure S4.**  $^{13}\text{C}$  NMR spectrum (175 MHz) of **1b** in  $\text{CDCl}_3$ .

**Table S1.** Absorbance data in different solvents.

Compound	Solvent	Absorption/ $\lambda_{\max}$ [nm]( log $\epsilon$ [M <sup>-1</sup> cm <sup>-1</sup> ])
<b>1a</b>	Toluene	411 (4.75), 512 (3.76), 628 (4.06), 685 (4.11)
	Chloroform	409 (4.90), 512 (3.71), 626 (4.11), 680 (4.07)
	DCM	408 (5.29), 513 (4.22), 628 (4.49), 680 (4.47)
	THF	415 (5.02), 523 (3.89), 627 (4.24), 691 (4.18)
<b>1b</b>	Toluene	406 (5.38), 510 (4.21), 739 (4.73)
	Chloroform	409 (5.55), 511 (4.51), 745 (4.91)
	DCM	409 (5.36), 511 (4.35), 721 (4.75)
	THF	413 (5.35), 519 (4.34), 725 (4.88)
<b>aza-BODIPY-a</b>	Toluene	484 (3.87), 662 (4.79)
	DCM	481 (4.06), 655 (4.93)
	Chloroform	484 (4.15), 658 (5.03)
<b>aza-BODIPY-b</b>	Toluene	483 (4.00), 663 (4.93)
	DCM	481 (4.00), 657 (4.89)
	Chloroform	497 (4.09), 658 (4.92)
<b>Ir<sup>III</sup>(ttP)Ph</b>	Toluene	409 (5.41), 512 (4.28)
	DCM	409 (5.30), 516 (4.18)
	Chloroform	409 (5.27), 512 (4.17)

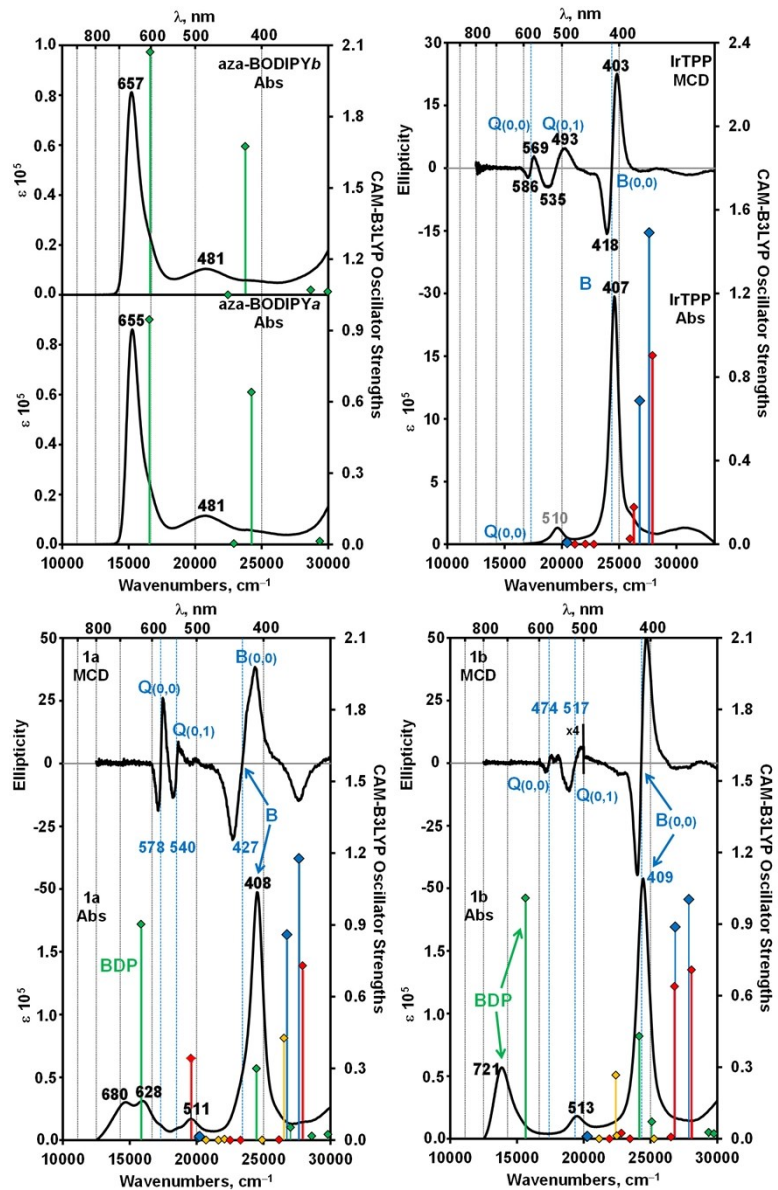


**Figure S5.** Absorption and MCD spectra of conjugates **1a**, **1b**, aza-BODIPY-a, aza-BODIPY-b and **Ir<sup>III</sup>(ttp)Ph** in dichloromethane. TD-DFT spectra calculated for B3LYP geometries with the CAM-B3LYP functional and 6-31G(d) basis sets are plotted against secondary axes. The TD-DFT calculations were performed in the presence of dichloromethane using the polarizable continuum model. Blue diamonds are used to highlight the Q and B bands of the  $\pi$ -system of the Ir(ttp) moiety, while green diamonds are used to highlight transition associated with the aza-BODIPY  $\pi$ -system. Red and yellow diamonds are used to highlight transitions involving the 5d orbitals of the Ir(III) ion and charge transfer transitions between the Ir<sup>III</sup>(tpp) and aza-BODIPY moieties, respectively. Vertical blue lines are used to highlight the crossover points of the pseudo- $A_1$  terms in the MCD spectra that are associated with the Q and B bands of Gouterman's 4-orbital model.<sup>1</sup>

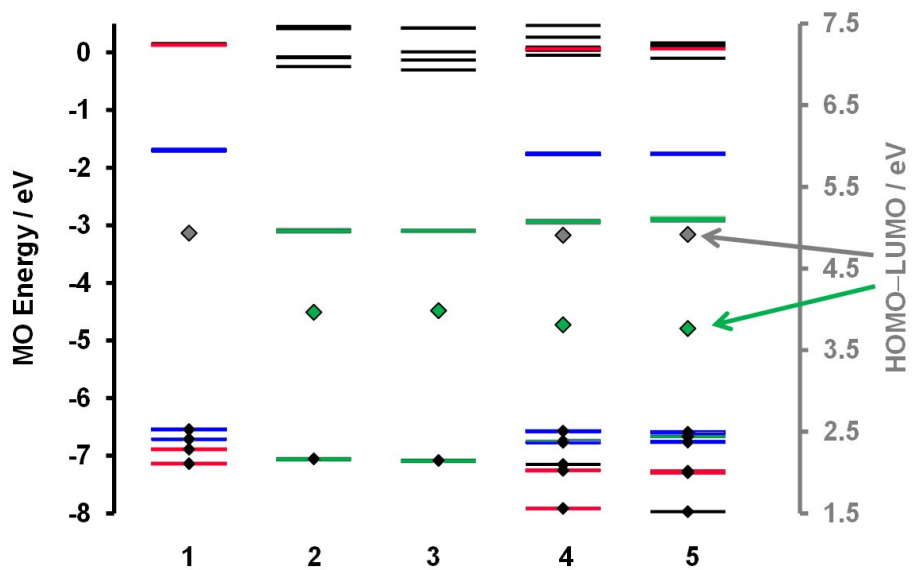


**Figure S6.** MO energies of Ir<sup>III</sup>(ttp)Ph (1), aza-BODIPY-a (2), aza-BODIPY-b (3), 1a (4) and 1b (5). TD-DFT calculations were performed in the presence of dichloromethane using the polarizable continuum model. The HOMO–LUMO gaps for the BODIPY and Ir<sup>III</sup>(ttp) moieties are plotted against a secondary axis and are denoted with large green and gray diamonds, respectively. The four frontier  $\pi$ -MOs of the  $\pi$ -system of the Ir<sup>III</sup>(ttp) moiety are highlighted with blue lines, while red and green lines are used to denote the 5d orbitals of the Ir(III) ion and the HOMO and LUMO of the aza-BODIPY  $\pi$ -system, respectively. Small black diamonds are used to highlight occupied MOs.

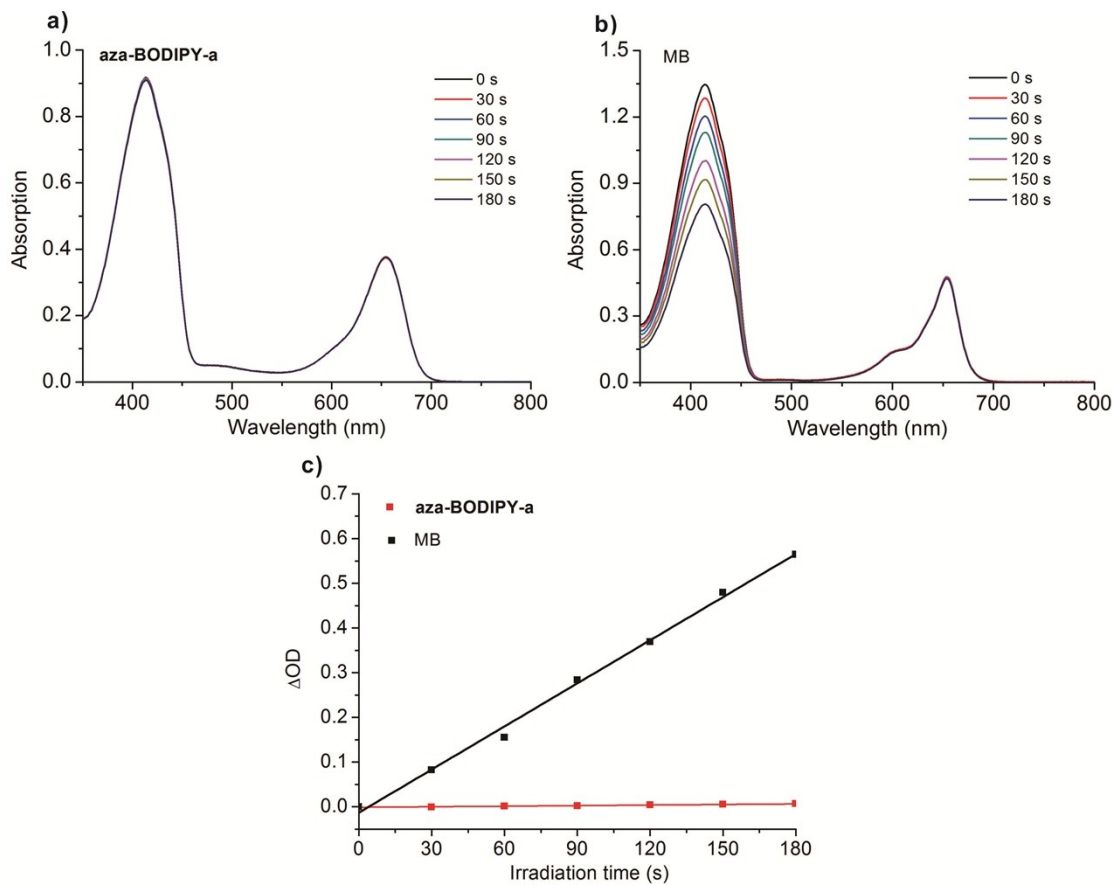


**Figure S7.** a) Absorption spectra of DPBF measured at 30 s intervals upon irradiation ( $\lambda_{\text{irr}} = 671$  nm) in the presence of  $4.5 \times 10^{-6}$  M **aza-BODIPY-a**; b) Absorption spectra of DPBF measured at 30 s intervals upon irradiation ( $\lambda_{\text{irr}} = 671$  nm) in the presence of MB; c) Plot of the change in the DPBF absorbance at 410 nm versus irradiation time in the presence of **aza-BODIPY-a** against MB as a standard in air-saturated dichloromethane.

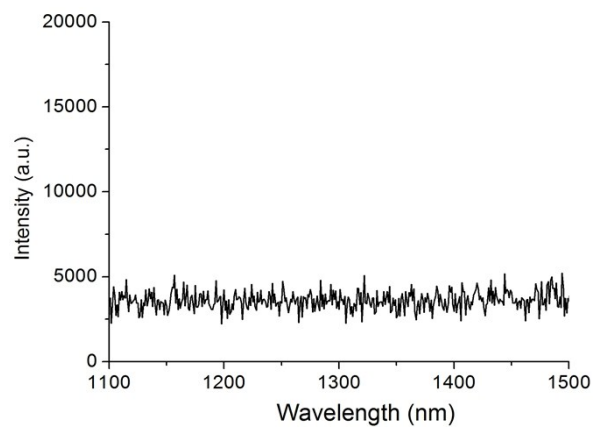


**Figure S8.** The  $^1\text{O}_2$  phosphorescence spectrum of **aza-BODIPY-a** in air-saturated dichloromethane upon irradiation with 650 nm ( $c = 4.5 \mu\text{M}$ , 298 K).

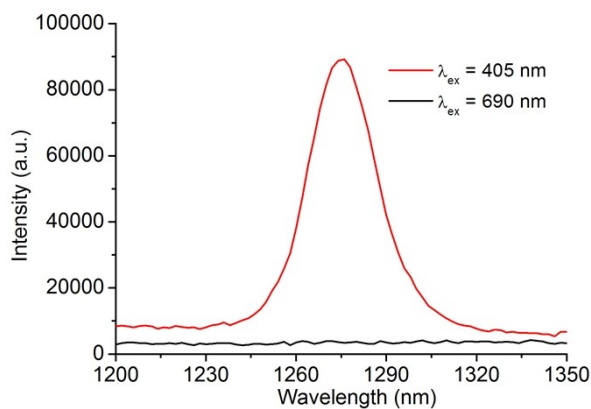


**Figure S9.** The  $^1\text{O}_2$  phosphorescence spectra of  $\text{Ir}^{\text{III}}(\text{ttp})\text{Ph}$  in air-saturated dichloromethane upon irradiation with 405 (red) and 690 nm (black) laser light ( $c = 5.0 \mu\text{M}$ , 298 K).

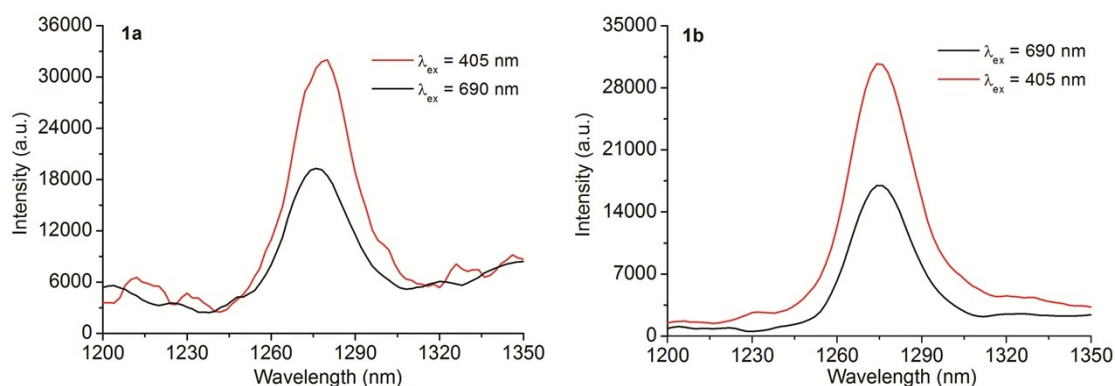


**Figure S10.** The  $^1\text{O}_2$  phosphorescence spectra of **1a** ( $c = 5.0 \mu\text{M}$ ) and **1b** ( $c = 5.0 \mu\text{M}$ ) in air-saturated dichloromethane upon irradiation with 405 (red) and 690 nm (black) laser light at room temperature.

**Table S2.** The ratios of singlet oxygen quantum yields ( $\Phi_\Delta$ ) upon irradiation with 405 nm and 690 nm of **1a**, **1b** in  $\text{O}_2$  saturated dichloromethane at 298 K.

Component	$\Phi_{\Delta(\lambda_{\text{ex}} = 405 \text{ nm})}/\Phi_{\Delta(\lambda_{\text{ex}} = 690 \text{ nm})}^a$
<b>1a</b>	0.95
<b>1b</b>	0.92

<sup>a</sup> The ratios of singlet oxygen quantum yields ( $\Phi_\Delta$ ) upon irradiation with 405 nm and 690 nm.<sup>2</sup>

## References

- 1 M. J. Frisch, G. W. Trucks, H. B. Schlegel, G. E. Scuseria, M. A. Robb, J. R. Cheeseman, G. Scalmani, V. Barone, B. Mennucci, G. A. Petersson, H. Nakatsuji, M. Caricato, X. Li, H. P. Hratchian, A. F. Izmaylov, J. Bloino, G. Zheng, J. L. Sonnenberg, M. Hada, M. Ehara, K. Toyota, R. Fukuda, J. Hasegawa, M. Ishida, T. Nakajima, Y. Honda, O. Kitao, H. Nakai, T. Vreven, J. A. Montgomery, J. E. Peralta, F. Ogliaro, M. Bearpark, J. J. Heyd, E. Brothers, K. N. Kudin, V. N. Staroverov, R. Kobayashi, J. Normand, K. Raghavachari, A. Rendell, J. C. Burant, S. S. Iyengar, J. Tomasi, M. Cossi, N. Rega, M. J. Millam, M. Klene, J. E. Knox, J. B. Cross, V. Bakken, C. Adamo, J. Jaramillo, R. Gomperts, R. E. Stratmann, O. Yazyev, A. J. Austin, R. Cammi, C. Pomelli, J. W. Ochterski, R. L. Martin, K. Morokuma, V. G. Zakrzewski, G. A. Voth, P. Salvador, J. J. Dannenberg, S. Dapprich, A. D. Daniels, Ö. Farkas, J. B. Foresman, J. V. Ortiz, J. Cioslowski, D. J. Fox, Gaussian 09, Revision D.01, Gaussian, Inc., Wallingford CT, 2009.
- 2 B. Marydasan, A. K. Nair, D. Ramaiah, *J. Phys.Chem. B*, 2013, **117**, 13515.